Tomasz RYMARCZYK[1,2], Grzegorz KŁOSOWSKI[3]

University of Economics and Innovation (1), Research & Development Centre Netrix S.A. (2), Lublin University of Technology (3)

doi:10.15199/48.2019.05.13

EIT detection methods of damage in landfills and flood embankments

***Abstract**. This paper presents a method examining landfills and flood embankments using electrical impedance tomography (EIT). Numerical and optimization methods were based on hybrid algorithms included neural networks connected with one of 3 statistical methods: generalized linear regression (GLR), generalized linear regression with stepwise regression (GLR-SR) and ElasticNET. The discussed techniques can be applied to the solution of inverse problems in EIT. The algorithms to identify unknown internal conductivities of the tested objects were implemented.*

***Streszczenie.** W artykule przedstawiono metodę badania uszkodzeń składowisk odpadów płynnych i wałów przeciwpowodziowych za pomocą elektrycznej tomografii impedancyjnej (EIT). Metody numeryczne i optymalizacyjne oparto na algorytmach hybrydowych obejmujących sieci neuronowe połączone z jedną z 3 metod statystycznych: uogólnioną regresją liniową (GLR), uogólnioną regresją liniową z regresją krokową (GLR-SR) oraz ElasticNET. Omówione techniki można zastosować do rozwiązania problemów odwrotnych w EIT. Zastosowane algorytmy umożliwiają identyfikację nieznanych wartości konduktancji wnętrza badanych obiektów. (**Metody EIT do wykrywania uszkodzeń składowisk i wałów przeciwpowodziowych**).*

Keywords: electrical tomography, flood embankments, landfills, neural networks, numerical modelling.
Słowa kluczowe: tomografia elektryczna, wały przeciwpowodziowe, składowiska odpadów, sieci neuronowe, modelowanie numeryczne.

Introduction

The presented article describes a group of innovative methods enabling the identification of damage to landfills and flood embankments. These are methods based on electrical impedance tomography (EIT) [1], however, significantly improved by using original algorithms that enable reconstruction of tomographic images. In this study, three types of hybrid algorithms were considered:

- generalized linear regression (GLR) [2],
- generalized linear regression with stepwise regression (GLR-SR),
- ElasticNET [3].

All three of the above statistical methods were used to reduce the number of predictors. In the considered EIT system, the input vector consists of 192 values of voltage drops taken due to the arrangement of 16 electrodes. The input vector reduced in this way was further used to train the artificial neural networks system (ANN) [4].

Among the tomographic methods, apart from the EIT, one can also be distinguished: electrical capacitance tomography [5-9], magnetoacoustics [10], multipath tomography [11] and others. In order to improve the imaging quality, various methods are used, mostly based on modern information techniques: fuzzy logic [12], GPU parallel computing [13], integer linear programming [14], etc.

Flood is one of the most common and frequent natural disasters. Floods are the cause of many human dramas. One of the ways to protect the floodplains near landfills, rivers and water banks is to lift flood embankments. Thanks to this, you can temporarily raise the level of freshet over the main river bed and suppress the flood. However, higher water level accelerates the erosion of the top of the embankment or landfill barrier and can destroy it. In addition, given the insufficient filtration power of the embankment body, high water can lead to an increase in the number of leaks, which may lead to partial destruction of the flood bank. Despite significant achievements in the design of safe bunds, unexpected changes may occur. That is why ongoing research is being carried out to develop a cheap and reliable tool that allows effective monitoring of embankments and dams. [15]

Among all methods of landfills and flood embankments faults detection, you can mention: deformation surveying (detecting deformation of the structure through manual measurements and automatic using micro-mirrors), visual assessment of technical condition (direct observation conducted by employees), geotechnical monitoring (detection of anomalies under construction geological foundation of the dam and landfill by deep drilling and probes), seismic monitoring (detection of building stability disturbances by means of accelerometer sensors that are excited whenever they identify vibrations of a certain level), hydrogeological monitoring (detection of anomalies caused by soaking the dam by observing piezometric pressures) in piezometers installed in the waste mass, on dams and near and far foreground), information systems for the analysis of large data sets. Additionally, hydrological monitoring (leakage detection) and chemical monitoring (detection of contamination of surrounding groundwater).

Most of the methods listed above are invasive or surface methods. Invasive methods involve the necessity of physical interference in the structure of the examined objects, which reduces the safety of their operation. Geodetic monitoring does not allow penetration into the structure of the flood embankment. Other methods, such as hydrological or chemical monitoring, make it possible to identify the threat too late - when the effects of the threat are already visible.

The EIT due to its non-destructive nature and the possibility of obtaining an image of the interior cross-section of the dam, is very attractive in comparison with traditional methods. The main reason for its low, hitherto prevalence is the difficulty in obtaining high resolution images in the case of cross-sections of large technical facilities such as landfills protections, embankments, flood banks and dams. During the research described in this article, the priority was first of all image quality (high resolution), as well as the speed of obtaining a tomographic image.

The effect of the research was to develop and compare 3 hybrid methods of processing tomographic signals: GLR+ANN, GLR-SR+ANN and ElasticNET+ANN.

The main advantages of the proposed EIT imaging system are: non-invasive and non-destructive measurement of the tested object [4, 16-19], the ability to display moisture distribution not only on the surface, but also inside the tested object, the ability to determine the dynamics of the leak propagation. The described research uses simulation tools based on the Matlab scientific software. A special role was played by the EIDORS toolkit working with the Matlab

software. It has been used to model cross-sections and topological algorithms using the finite element method to solve the inverse problem. [10]

Materials and methods

On the basis of observations of real technical objects like dams and dams, a physical model was made in the field. Fig. 1 shows a top view of a flood embankment model with 16 electrodes arranged in a row.

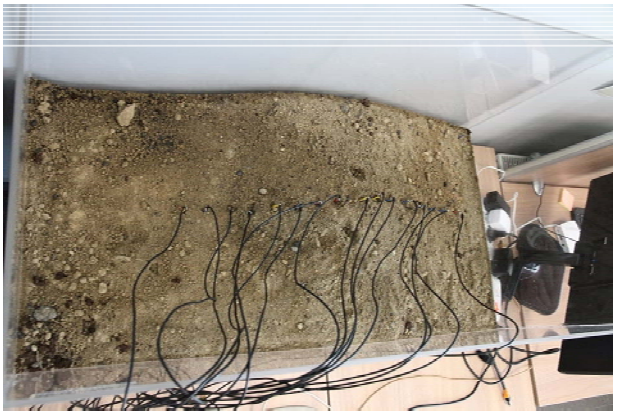

Fig.1. The physical model of the flood embankment with the arrangement of 16 electrodes

Fig. 2 shows the model of the EIT system. Each reconstruction event includes 192 voltages generated by a set of 16 electrodes. Then, the vector 192 values powers each of the 9853 neural subsystems. The number of substrings is equal to the resolution of the output image grid, which in the case study is 9853. Each subsystem generates one real value, which is the color of the given output pixel. The entire reconstructed 3D image consists of 9853 pixels.

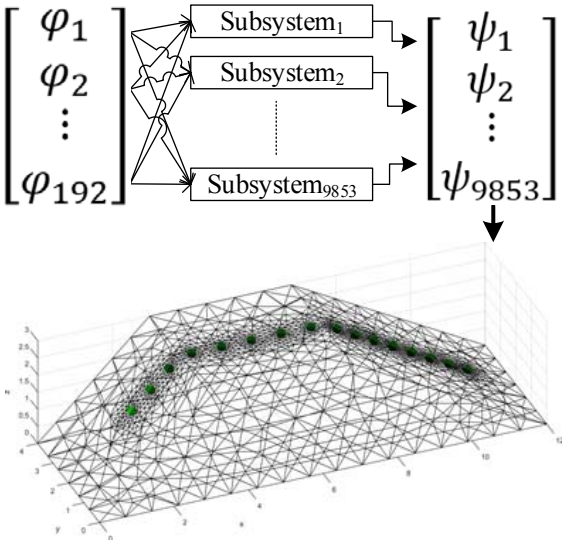

Fig.2. Model of the EIT system converting electrical signals into 3D images

EIT determines the recovery of the conductivity of the interior of the examined object from a knowledge of currents and voltages applied to its surface. The neural architecture of the proposed innovative intelligent imaging system ensures higher-resolution images of the cross-section of the scanned object. The novelty of the proposed flood embankment monitoring system that distinguishes it from previous solutions lies in the use of a unique system of interconnected hybrid neural networks. The innovative concept for tomographic image reconstruction was dictated by the need to improve reconstructed image resolution, as well as to increase the sensitivity of the monitoring system to changes occurring inside the flood embankment.

Due to the large number of predictors (192) per single pixel of the image, training of ANN is difficult. Neural network is easily over-trained then. In addition, the network training time is significantly longer and the network is susceptible to noise. To avoid the above problems, three methods of reducing the number of predictors were tested: GLR, GLR-SR and ElasticNET.

Formula (1) shows the vector 192 of the predictor values.

$$X = [x_1, x_2, ..., x_{192}] \tag{1}$$

where: x – predictors.

The generalized linear model determines the (linear) relation between the dependent variable (or response) Y and the set of predictors (explanatory variables) X, in the form:

$$Y = b_0 + b_1 X_1 + b_2 X_2 + ... + b_k X_k \tag{2}$$

In equation (2), b_0 is the regression coefficient for a free word, and b_i is the regression coefficients for variables (numbers from 1 to k), calculated on the basis of data.

Table 1 shows the reduced predictor vector for the pixel ψ_{2000} using generalized linear regression with stepwise regression (GLR-SR) method. The predictor's rejection criterion was: *PValue<0.5* and *FStat>0.5*. The *PValue* is the probability of getting a result at least as extreme as the one that was actually observed, given that the null hypothesis is true. The *PValue* is a probability, while the *F* ratio is a test statistic, calculated as:

$$FStat = \frac{Var_{between}}{Var_{error}} \tag{3}$$

where: $Var_{between}$ - variance of the group means (Mean Square Between); Var_{error} - mean of the within group variances (Mean Squared Error).

Table 1. Estimated coefficients

Input value	Deviance	FStat	PValue
x_{53}	41.084967	1824.0739	$7.432749 \cdot 10^{-102}$
x_{66}	27.4241	76.5705	$9.76549 \cdot 10^{-16}$
x_{115}	21.716	11.4594	0.000860870
x_{117}	20.1066	9.3465	0.002552590
x_{141}	21.0854	5.7720	0.017231300

As Table 1 indicates, out of 192 values of the input vector, after the reduction of GLR-SR there are 5 selected predictors: x_{53}, x_{66}, x_{115}, x_{117}, x_{141}. Linear predictor formula for pixel ψ_{2000}:

$$y_{2000} = 1 + x_{53} + x_{66} + x_{115} + x_{117} + x_{141} \tag{4}$$

Fig. 3 shows the slice plot of the responses for pixel ψ_{2000}. All 5 lines illustrating the influence of a given predictor on the output pixel value are not horizontal. This means that their change has a significant impact on the output variable. The more vertical the course of the input variable in a given range of values, the greater its impact on the result.

This plot shows the main effects for all predictor variables. The green line in each panel shows the change in the response variable as a function of the predictor variable when all other predictor variables are held constant. The dashed red curves in each panel show the 95% confidence bounds for the predicted response values. The horizontal dashed blue line in each panel shows the predicted response for the specific value of the predictor variable corresponding to the vertical dashed blue line.

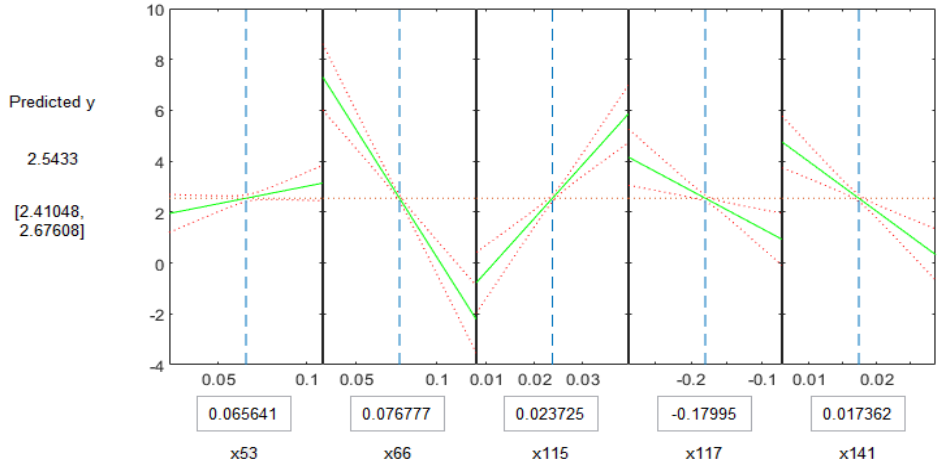

Fig.3 Slice plot of the responses

Fig. 4 shows a histogram of residuals for all cases used in the process of vector reduction of predictors. The most deviations have values close to zero, and the graph resembles a normal distribution curve. This is good evidence of the quality of the reduction process.

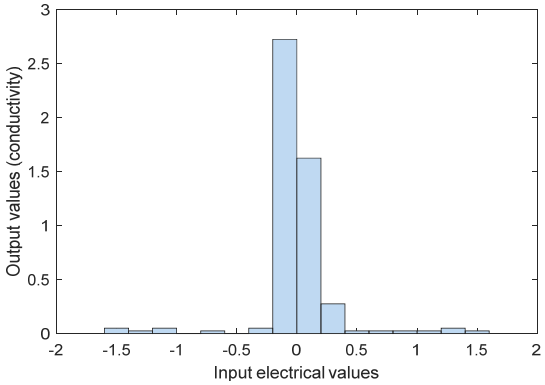

Fig.4. Histogram of residuals

The normal probability scatter plot of residuals was shown in Fig. 5.

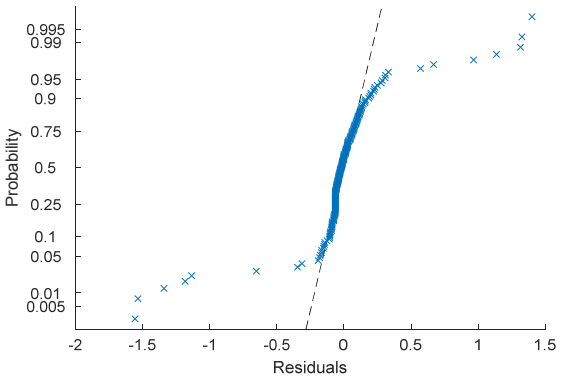

Fig.5. Normal probability plot of residuals

The distribution of observations on the graph indicates that the most frequent deviations belong to the range -0.1 to 0.1. Since the most points of observation are in the immediate vicinity of the zero value, the graph confirms the effectiveness of the process of reducing the number of predictors.

In the same way as the GLR-SR method was used, the predictors were reduced using the GLR and ElasticNET methods. The input data transformed in this way was used to train three artificial neuron network systems (ANN). All of the ANNs used had one hidden layer consisting of 9 neurons and one neuron in the output layer.

Fig. 6 shows a single neural network model generating pixel ψ_{2000} in a reconstructed image grid. In this case, the reduction of predictors was performed using the ElasticNET method, hence the number of input variables is 38.

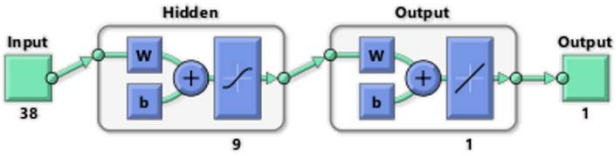

Fig.6. Model of a single neural network for pixel ψ_{2000} in ElasticNET+ANN hybrid model

Results and conclusions

In Figure 7, we see the first four drawings, the upper one is the pattern. the other three drawings below are reconstructions made sequentially with all three hybrid methods. The colored scale placed on the right side of the drawings determines the conductance values of individual pixels on the grid of the reconstructed output image. Comparing the reconstructions of all three hybrid methods: generalized linear regression (GLR), generalized linear regression with stepwise regression (GLR-SR) and ElasticNET, it can be concluded that the best results were obtained using the ElasticNET method. The weakest results were obtained using the GLR method.

despite the visible differences, it should be noted that all three hybrid methods function well enough to clearly identify threats arising inside the flood embankment. When analyzing the reasons for differences in the operation of individual hybrid methods, it should be taken into account that each method requires individual selection of penalty rates, or in the case of ElasticNET, a factor determining the impact of LASSO (low absolute shrinkage and selection operator) and ridge regression. It is very likely that in the case of other selection of penalty rates, other methods could work better. It is also worth noting that in the case of Elastic net, the number of predictors after reduction was much greater than eg in the case of the GLR-SR method (38 predictors in ElastinNET versus 5 predictors of GLR-SR).

The results of the conducted research confirm that combining statistical methods with artificial neural networks can be an effective solution when creating hybrid methods that improve previously used EIT techniques. The concept of creating neural network systems from which each individual network generates its own pixel of the output

image is an effective method of creating two- and three-dimensional tomographic reconstructions.

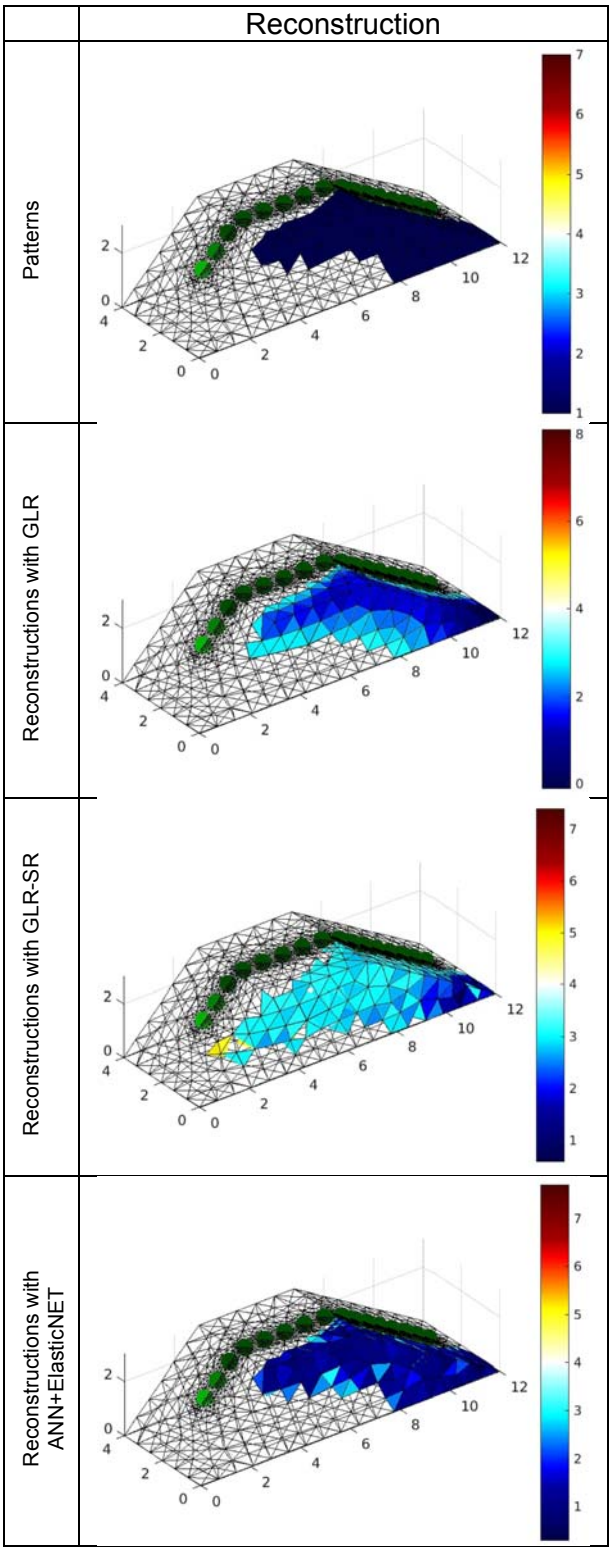

Fig.7. Comparison of simulation results for all tested hybrid methods

***Authors**: Tomasz Rymarczyk, Netrix S.A., Phd. Eng, Research and Development Centre, Związkowa 26, 20-148 Lublin, University of Economics and Innovation in Lublin, ul. Projektowa 4, 20-209 Lublin, e-mail: tomasz@rymarczyk.com; Grzegorz Kłosowski, Ph.D. Eng., Lublin University of Technology, Nadbystrzycka 38A, Lublin, Poland,*
E-mail: g.klosowski@pollub.pl.

REFERENCES

[1]. Filipowicz, S. F. & Rymarczyk, T. Measurement Methods and Image Reconstruction in Electrical Impedance Tomography. Przegląd Elektrotechniczny 88 (2012), 247–250.
[2]. Alhamzawi, R. & Ali, H. T. M. The Bayesian adaptive lasso regression. Mathematical Biosciences. (2018).
[3]. Zou, H. & Hastie, T. Regularization and variable selection via the elastic net. Journal of the Royal Statistical Society: Series B (Statistical Methodology). 67 (2005), 301–320
[4]. Rymarczyk, T., Kłosowski, G. & Kozłowski, E. A Non-Destructive System Based on Electrical Tomography and Machine Learning to Analyze the Moisture of Buildings. Sensors, 18 (2018), 2285
[5]. Wajman, R., Fiderek, P., Fidos, H., Jaworski, T., Nowakowski, J., Sankowski, D., & Banasiak, R. Metrological evaluation of a 3D electrical capacitance tomography measurement system for two-phase flow fraction determination. Measurement Science and Technology. 24 (2013), no. 6, 065302
[6]. Kryszyn, J. & Smolik, W. Toolbox for 3d modelling and image reconstruction in electrical capacitance tomography. Informatyka, Automatyka, Pomiary w Gospodarce i Ochronie Środowiska. (IAPGOŚ), 7 (2017), no 1, 137-145
[7]. Kryszyn, J., Wanta, D. M. & Smolik, W. T. Gain Adjustment for Signal-to-Noise Ratio Improvement in Electrical Capacitance Tomography System EVT4. IEEE Sensors Journal. 17 (2017), 8107–8116.
[8]. Garbaa, H., Jackowska-Strumiłło, L., Grudzień, K. & Romanowski, A. Application of electrical capacitance tomography and artificial neural networks to rapid estimation of cylindrical shape parameters of industrial flow structure. Archives of Electrical Engineering. 65 (2016), 657–669
[9]. Grudzien, K., Chaniecki, Z., Romanowski, A., Sankowski, D., Nowakowski, J., & Niedostatkiewicz, M. Application of twin-plane ECT sensor for identification of the internal imperfections inside concrete beams. Instrumentation and Measurement Technology Conference Proceedings (I2MTC) (2016), 7520512
[10]. Ziolkowski, M., Gratkowski, S. & Zywica, A. R. Analytical and numerical models of the magnetoacoustic tomography with magnetic induction. COMPEL-The international journal for computation and mathematics in electrical and electronic engineering. 37 (2018), 538–548
[11]. Polakowski, K., Filipowicz, S. F., Sikora, J. & Rymarczyk, T. Quality of imaging in multipath tomography. Przegląd Elektrotechniczny 85 (2009), no. 12, 134–136
[12]. Mazurkiewicz, D. Maintenance of belt conveyors using an expert system based on fuzzy logic. Archives of Civil and Mechanical Engineering. 15 (2015), 412–418
[13]. Dusek, J., Hladky, D. & Mikulka, J. Electrical impedance tomography methods and algorithms processed with a GPU. 2017 Progress In Electromagnetics Research Symposium - Spring (PIERS) (2017), 1710–1714
[14]. Kłosowski, G., Kozłowski, E. & Gola, A. Integer Linear Programming in Optimization of Waste After Cutting in the Furniture Manufacturing. International Conference on Intelligent Systems in Production Engineering and Maintenance, 637, (2018), 260-270
[15]. Rymarczyk, T. & Kłosowski, G. Application of neural reconstruction of tomographic images in the problem of reliability of flood protection facilities. Eksploat. i Niezawodn. -- Maint. Reliab. 20 (2018), no.3, 425–434
[16]. Psuj, G. Multi-Sensor Data Integration Using Deep Learning for Characterization of Defects in Steel Elements. Sensors 18 (2018), no. 1, 292
[17]. Lopato, P., Chady, T., Sikora, R., Gratkowski, S. & Ziolkowski, M. Full wave numerical modelling of terahertz systems for nondestructive evaluation of dielectric structures. COMPEL-The international journal for computation and mathematics in electrical and electronic engineering. 32 (2013), no. 3, 736–749
[18]. Rymarczyk T., Sikora J. Applying industrial tomography to control and optimization flow systems, Open Physics, 16 (2018); 332–345
[19]. Kryszyn J., Smolik W., Radzik B., Olszewski T., Szabatin R. Switchless charge-discharge circuit for electrical capacitance tomography, Measurement Science and Technology, 25 (2014), no. 11, 115009